VOL. 14, NO. 20, OCTOBER 2019 ISSN 1819-6608
ARPN Journal of Engineering and Applied Sciences

www.arpnjournals.com

CONTROL OF A SUPER-CAPACITORS AS ENERGY STORAGE WITH THIRTEEN-LEVEL INVERTER

Rosli Omar, Mohammed Rasheed, Marizan Sulaiman and Wahidah Abd Halim
Faculty of Electrical Engineering, Industrial Power, Universiti Teknikal Malaysia, Melaka, Malaysia
E-Mail: rosliomar@utem.edu.my

ABSTRACT

Control of a super-capacitors as energy storage with thirteen-level inverter is presented in this paper. A NR and PSO techniques are presented for selective harmonics elimination (SHE) solution in a modified Cascaded H Bridge Multilevel inverter (CHB-MLI). The Selective Harmonic Elimination Pulse-Width Modulation (SHE-PWM) is a powerful technique for harmonic minimization in multilevel inverter. The proposed design is used to charge the energy storage such as battery, super capacitor.NR and PSO techniques are used to determine the switching angles by solving the non-linear equation's analysis of the output voltage waveform of the modified CHB-MLI in order to control the fundamental component. The proposed techniques, based on NR and PSO techniques, are capable to minimize the Total Harmonic Distortion (THD) of output voltage of the modified CHB-MLI within allowable limits. A comparison has been made between NR and PSO techniques related to optimization in order minimize harmonic distortion based on super capacitor as super capacitor. The main aims of this paper cover design, modeling, construction and testing of a laboratory the modified topology of the CHB-MLI for a single-phase prototype for 13-levels. The experimental results of the prototype are also illustrated. The controllers based on NR and PSO are applied to the modified multilevel inverter based on super capacitor as super capacitor. The Digital Signal Processing (DSP) TMS320F2812 is used to implement these modified inverters control schemes using NR and PSO method. The proposed controller is then coded into a DSP TMS320F2812 board. The inverter offers much less THD using PSO scheme when compared with the NR scheme.

Key words: harmonics, PSO, modified multilevel inverters, digital signal processor DSP, 13 level.

INTRODUCTION

Multilevel power conversion was first introduced 25 years ago [1-5]. The general concept involves utilising a higher number of active semiconductor switches to perform the power conversion in small voltage steps. There are several advantages to this approach when compared with traditional two-level power conversion. The smaller voltage steps lead to the production of higher power quality waveforms and also reduce the *dv/dt* stresses on the load and the electromagnetic compatibility concerns. Another important feature of multilevel converters is that the semiconductors are wired in a series-type connection, which allows operation at higher voltages. However, the series connection is typically made with clamping diodes, which eliminate over voltage concerns. Furthermore, since the switches are not truly series connected, their switching can be staggered, which reduces the switching frequency and thus the switching losses. In order to lower harmonic content to improve the output waveform for voltage inverter, reduce the size of the filter utilized and the level of electromagnetic interference (EMI). Numerous topologies to realize this connectivity which can be generally divided into three major categories, namely, diode clamped MLI, flying capacitor MLI and separated dc sources cascaded H-bridge CHB-MLI. Type of MLI which using a single DC source rather than multiple sources is the diode-clamped MLI. While, FC type is designed by series connection of capacitor clamped switching cells. CHB switches are connected in parallel and series in order to provide high power demand and high-power quality [3]-[9]. For improving the quality of the output voltage inverter for two types of MLI, as symmetrical and asymmetrical, both types are very effective and efficient for multilevel inverter utilize reduced number of switching devices with Hybrid topologies for the conventional and non-conventional multilevel inverter topologies to create a specified number of output voltage levels in operating in higher voltage levels based on DC voltage supply [10] [11]. Reduced number of switches with installation area and cost and has simplicity of control system, with a high number of steps associated using a new topology of cascaded multilevel inverter (CHB-MLI) has been presented in [12]. A current source inverter (CSI) apply a new topology for multilevel with reduced number of switches to generate desired output current for multilevel based on sinusoidal pulse width modulation (SPWM) method. This topology employs (n+7)/2 switches and (n−1)/2current-sharing inductors for an n-level CSI has been developed in [13]. For 5-level single-phase inverter has been developed by field-programmable gate array (FPGA). The digital control technique is generated based on multi carrier PWM in Altera DE2 board, which has many features that allow design based on DC supply application of the system device have been implementation Simulation and experiment results in [14]. A seven-level inverter has been simulated via implementation of PWM techniques to reduce total harmonic distortion (THD). Therefore, with decrees number of gate driver in the circuit, there will be an increase for high voltage inverter. The circuitry consists DC supply and smaller (CHB-MLI) blocks connected in series to implementation its characteristic output waveform [15].

The energy SC as storage charged to applied modified CHB-MLIs. Important coding in order to control

the modified CHB-MLIs using NR and PSO techniques for optimisation of the output of the modified CHB-MLIs for 13-levels is also created and then embedded into DSP TMS320F2812. Most of the researchers applied PSO technique in a single phase of a conventional CHB-MLIs. The NR and PSO techniques are used to calculate switching angles with the capability to eliminate harmonics of the output CHB-MLIs. Finally, in this paper method is evaluated and validated through experimental results.

SUPER-CAPACITOR (SC) MODEL

A SC can be modeled by using some standard circuit components as shown in Figure-1. This circuit design is used because a similar circuit is presented in the datasheet for the SC from EPCOS and because of recommendations from the project supervisor [16]. SIMULINK is used to create the first model of the SC according to the basic circuit described in Figure-2. Initial model testing is done with a simple circuit consisting of a resistance in series with a capacitance and resistance in parallel. This base circuit manages to show the basic function of the SC [17]. By adding more components until the circuit described in Figure-1 is achieved, the accuracy of the model is improved. The SIMULINK model used as the basic model of the SC is shown in Figure-2. The relay block controls the switch that connects the balancing resistance R3 to the circuit [17].

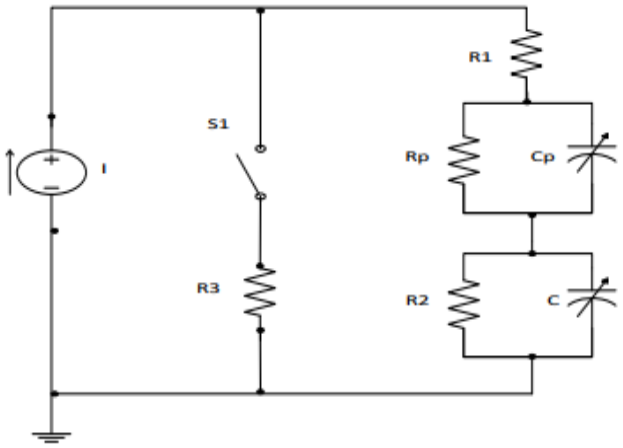

Figure-1. The basic circuit model of the SC (EPOCS).

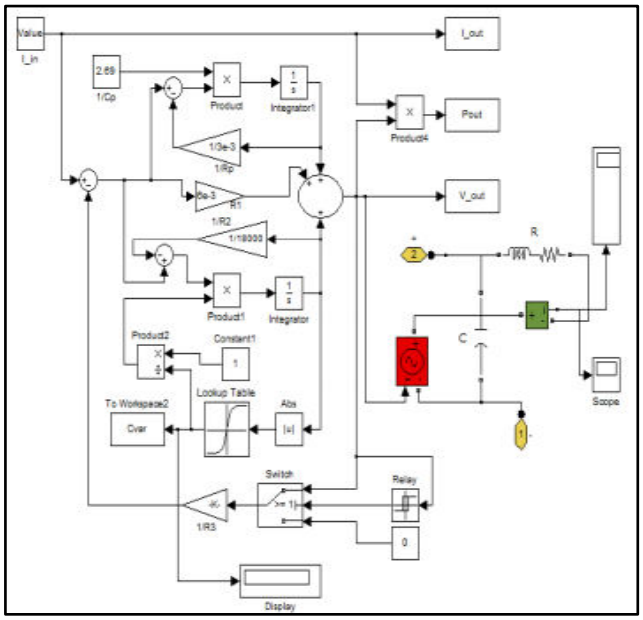

Figure-2. Simulink model of SC.

A. Main Capacitance

The capacitance value can be calculated in two different ways. The first method is to look at the voltage derivative during the charging of the super-capacitor (SC). The relation between voltage derivative and the capacitance is:

$$(t) = C\frac{d}{dt}\,u(t) \qquad (1)$$

Where;

C = the capacitance. Using this relation, the capacitance can be calculated for different parts of the voltage curve. When high currents are used, other effects than the capacitance can affect the voltage level. These effects can cause the calculated capacitance value to be incorrect.

SWITCHINGOPERATION MODES OF MODIFIEDCHB-MLIS FOR 13-LEVELS

The block diagram of modified CHB-MLIs with SC source based on controller PSO algorithm is shown in Figure-3. The switching mode operation of the proposed of a single-phase modified CHB-MLIs for 13-levels is illustrated in Figure-4. As previously mentioned, the proposed topology adopts a full-bridge configuration with an auxiliary circuit comprising four diodes and a switch, and generates half-level DC bus voltage. To depict each switch's switching pattern, Figure-5 shows the timing diagram or switching pattern of modified CHB-MLIs. The Output voltages of modified CHBMLIs for 13-levels can be summarized as described in Table-1. As a solution, this work presents a 13-level PWM inverter with output voltages Vdc, Vdc/2, Vdc/3, Vdc/4, zero, -Vdc/4, -Vdc/3, -Vdc/2 and -Vdc. Increased number of output levels reduces harmonic content.

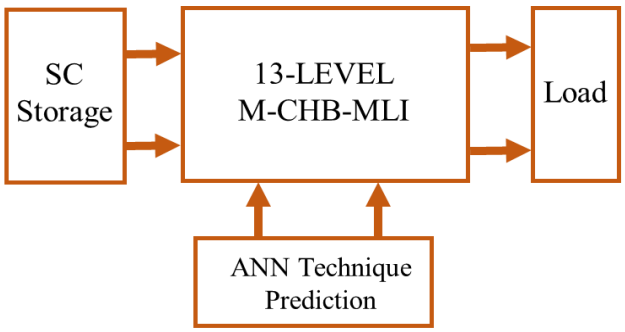

Figure-3. Block diagram of a modified CHB-MLIs with SCsource using PSO algorithm.

Table-1. Output voltage for 13-level to the switches' On=1-Off=0 condition.

Voltage State	S_1	S_2	S_3	S_4	S_5	S_6	S_7	S_8	S_9	S_{10}	S_{11}	S_{12}	S_{13}	S_{14}	S_{15}	Vo
A	1	0	0	1	0	1	0	0	1	0	1	0	0	1	0	Vdc
B	1	0	0	1	0	1	0	0	1	0	0	0	0	1	1	$V_{dc}/2$
C	1	0	0	1	0	0	0	0	1	1	0	0	0	1	1	$V_{dc}/3$
D	0	0	0	1	1	0	0	0	1	1	0	0	0	1	1	$V_{dc}/4$
E	0	0	0	1	1	0	0	0	1	1	0	0	1	1	0	$V_{dc}/5$
F	0	0	0	1	1	0	0	1	1	0	0	0	1	1	0	$V_{dc}/6$
G	0	0	1	1	0	0	0	1	1	0	0	0	1	1	0	0
H	1	1	0	0	0	1	1	0	0	0	1	1	0	0	0	0*
I	0	1	0	0	1	1	1	0	0	0	1	1	0	0	0	$-V_{dc}/6$
J	0	1	0	0	1	0	1	0	0	0	1	1	0	0	1	$-V_{dc}/5$
K	0	1	0	0	1	0	1	0	0	1	0	1	0	0	1	$-V_{dc}/4$
L	0	1	1	0	0	0	1	0	0	1	0	1	0	0	1	$-V_{dc}/3$
M	0	1	1	0	0	0	1	1	0	0	0	1	0	0	1	$-V_{dc}/2$
N	0	1	1	0	0	0	1	1	0	0	0	1	1	0	0	-Vdc

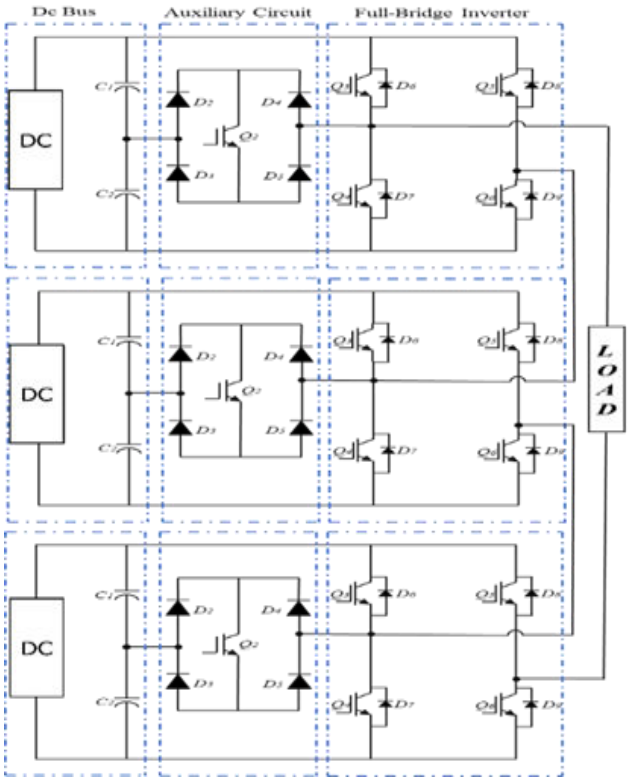

Figure-4. Proposal Modified of a CHB-MLI, Single-Phase 13-level Topology.

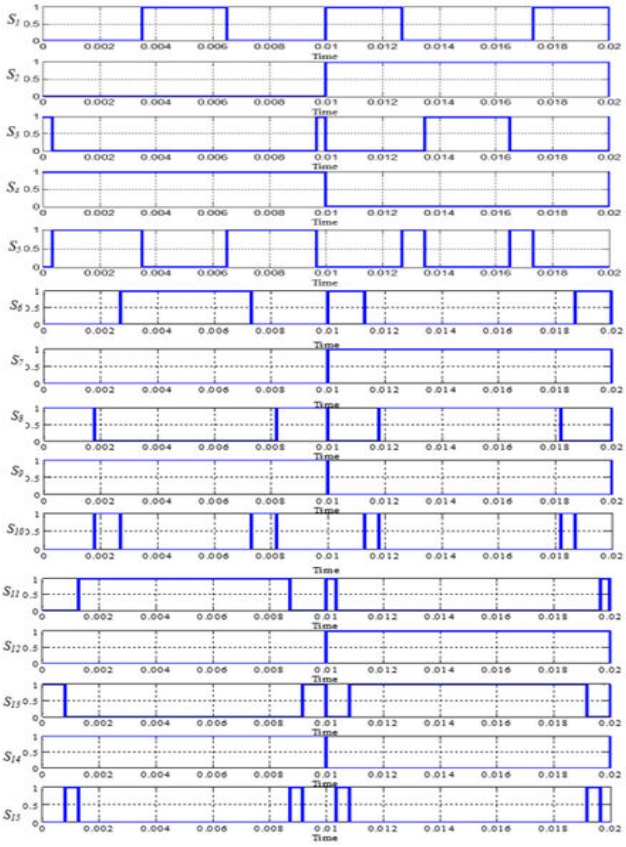

Figure-5. Switching pattern of modified CHB-MLIs for 13-Levels.

Analyses of the Proposed Topologies of a Modified CHB-MLIS for 13-Levels

A. Fourier series for Output Voltage of Proposed of a Modified CHB-MLIs for 13-Level

The equations for 13-levels based on the Fourier series are described below [18]:

$$f(t) = f_{\theta 1}(t) + f_{\theta 2}(t) + f_{\theta 3}(t) + f_{\theta 4}(t) + f_{\theta 5}(t) + f_{\theta 6}(t)$$

$$= \sum_{n=1,2,5}^{\infty} \frac{2Vdc}{n\pi}(V_{dc1}\cos(n\alpha_1) + V_{dc2}\cos(n\alpha_2) + V_{dc3}\cos(n\alpha_3) + V_{dc4}\cos(n\alpha_4) + V_{dc5}\cos(n\alpha_5) + V_{dc6}\cos(n\alpha_6))\sin(nwt) \quad (2)$$

where:

Vdc : Voltage of each voltage source that was in unity

θi : The switching angles

From (2), four equations were resulted in eliminating the 1st, 3th, 5th, 7th, 9th and 11th harmonic.

$$V_{AN} = V_{dc1} + V_{dc2} + V_{dc3}$$

$$b_n = \frac{2V_{dc}}{\pi}\left\{\begin{matrix}\cos(n\alpha_1) + \cos(n\alpha_2) + \cos(n\alpha_3) + \cos(n\alpha_4) + \\ \cos(n\alpha_5) + \cos(n\alpha_6)\end{matrix}\right\} n = 1,3,5,7,.. \quad (3)$$

Eq. (2) has *s* variables ($\theta_1, \theta_2, \theta_3, \ldots, \theta_s$), where $0 < \theta_1 < \theta_2 < \theta_3 \ldots < \theta_s < \pi/2$, and a solution set is obtained by assigning a specific value to the fundamental component, V_f, and equating s-1 harmonics to zero as given below:

$$V_1\cos(\theta_1) + V_2\cos(\theta_2) + V_3\cos(\theta_3) + V_4\cos(\theta_4) + V_5\cos(\theta_5) + V_6\cos(\theta_6) = 6m$$
$$V_1\cos(3\theta_1) + V_2\cos(3\theta_2) + V_3\cos(3\theta_3) + V_4\cos(3\theta_4) + V_5\cos(3\theta_5) + V_6\cos(3\theta_6) = 0V_1\cos(5\theta_1) + V_2\cos(5\theta_2) + V_3\cos(5\theta_3) + V_4\cos(5\theta_4) + V_4\cos(5\theta_4) + V_4\cos(5\theta_4) = 0$$
$$V_1\cos(7\theta_1) + V_2\cos(7\theta_2) + V_3\cos(7\theta_3) + V_4\cos(7\theta_4) + V_5\cos(7\theta_5) + V_6\cos(7\theta_6) = 0V_1\cos(9\theta_1) + V_2\cos(9\theta_2) + V_3\cos(9\theta_3) + V_4\cos(9\theta_4) + V_5\cos(9\theta_5) + V_6\cos(9\theta_6) = 0$$
$$V_1\cos(11\theta_1) + V_2\cos(11\theta_2) + V_3\cos(11\theta_3) + V_4\cos(11\theta_4) + V_5\cos(11\theta_5) + V_6\cos(11\theta_6) = 0 \quad (4)$$

where $m = V_f/(2Vdc/\pi)$, and it is related to the modulation index *mi* by $mi = m/s$, where $0 < mi < 1$. An objective function is then needed for the optimisation procedure selected as a measure of effectiveness of eliminating selected order of harmonics while maintaining the fundamental component at a pre-specified value. Therefore, this objective function is defined as:

$$F(\theta_1, \theta_2, \ldots, \theta_s) = \left[\sum_{n=1}^{s} V_1\cos(\theta_n) - m\right]^2 + \left[\sum_{n=1}^{s} V_2\cos(3\theta_n)\right]^2 + \ldots \left[\sum_{n=1}^{s} V_s\cos(2s-1)\theta_s\right]^2 \quad (5)$$

The optimal switching angles are obtained by minimising equation (5) subject to the constraint $0 < \theta_1 < \theta_2 < \theta_3 < \theta_4 \_ < \theta_s < \pi/2$, and consequently the required harmonic profile is achieved. The main challenge is the non-linearity of the transcendental set of Eq. (5), as most iterative techniques can be used with five and 13-levels of the modified CHB-MLIs as shown in Figure-6 and each step is explained below:

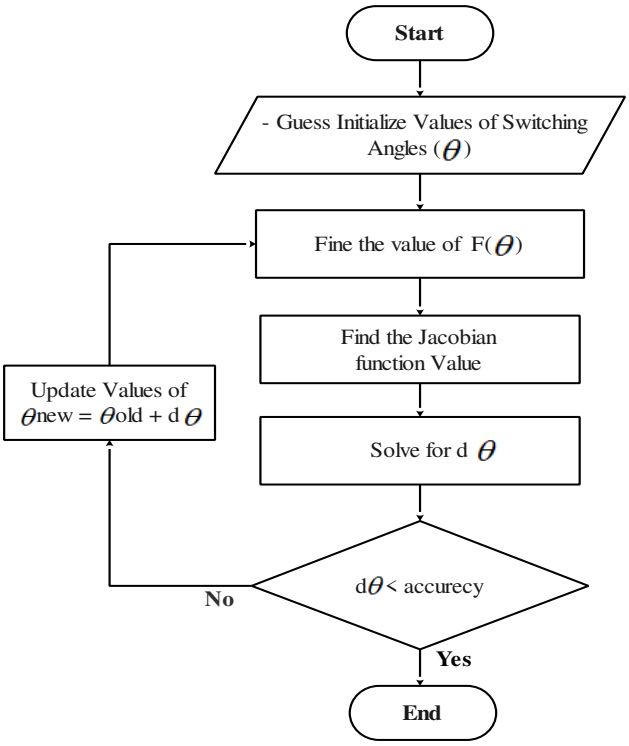

Figure-6. General flow-chart of NR of the modified CHB-MLIs.

A. NR Technique

The values of the conducting angles $\theta_1, \theta_2, \theta_3, \theta_4, \theta_5$, and θ_6 can be chosen by solving the transcendental equations using a modulation index formula equation (6) to obtain the suitable.

$$M = \frac{\pi V f}{2V_{dc}} \ (0 \le M \le 1) \quad (6)$$

Where, modulation index values, m_i. Other angles which are θ_7 until θ_{24} can be obtained by referring the output waveform of 13-levels of a modified CHB-MLIs theory in Figure-7. The procedure of detecting attributes and configuration of a system is called optimisation. For 13-level inverter single phase, only five harmonics can be eliminated here which are the 3rd, 5th, 7th, 9th, and 11th harmonics, chosen to be removed. Thus, the switching angle can be found by solving transcendental equations by using NR technique. Which is the output voltage for 13-level of a modified CHB-MLIs. These switching angles are then examined for their corresponding THD given by:

$$THD_V = \frac{\sqrt{\sum_{n=1}^{\infty} V_n^2}}{V_1} \quad (7)$$

The effect of optimised angles for 13-levels are $\alpha_1, \alpha_2, \alpha_3, \alpha_4, \alpha_5, \alpha_6$, on the THD and the modulation index is shown in Figure-7. By using MATLAB coding for number of iterations it can be easily concluded that the modulation index equal 0.949. However, the THD value of 13-levels equal to 6.18 %.

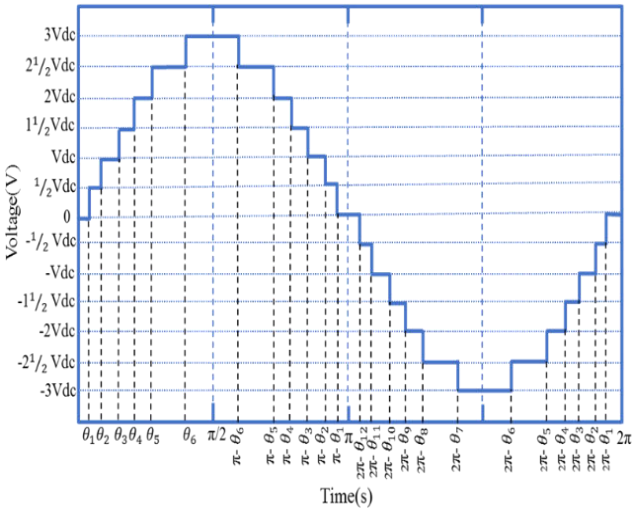

Figure-7. Vab at low switching frequency of modified CHB-MLIs, for 13-levels.

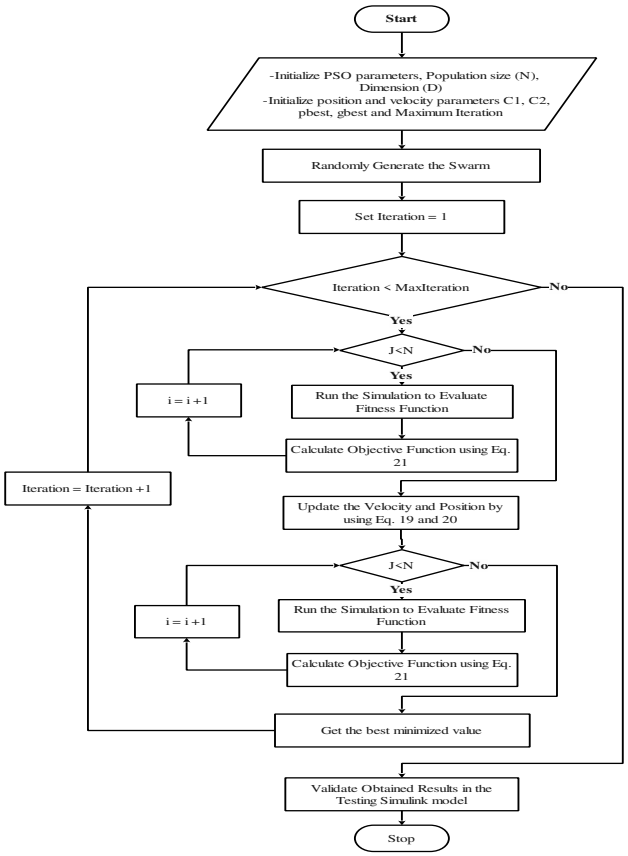

Figure-8. General flow chart of PSO of a modified CHB-MLIs.

B. Particle Swarm Optimization PSO Technique

PSO has become a very popular technique in solving non-linear optimization problems. Many types of evolutionary algorithms; particle swarm is preferred primarily because of its computational efficiency, simplicity and ability to avoid local optima. PSO has the several key advantages over other evolutionary optimization techniques [19]-[22]. The PSO algorithm is required to solve nonlinear equations based on SHE algorithm for solving the transcendental equations in order to optimise best switching angles. The number of iteration algorithm is solved using MATLAB coding to get better angles and harmonic. From number of iteration PSO algorithm.

Step 1 Initialise the system parameters such as velocity vector Vi, location vector Xi, personal best particle vector Pi, particle inertia weight C0, and global best vector Pg. Assign the values of generations as 100, population size as 40, cognitive parameter C1 as 0.5 and social parameter C2 as 1.25.

Step 2 Check for the case 0 < (C1 + C2) < 2 and (C1 + C2)/ 2 < C0 < 1, if the two cases are satisfied then the system will be guaranteed to converge to a stable equilibrium point. If false, go to Step 1.

Step 3 Update the Velocity, Vi (t + 1).

$$\text{Vij (t+1)} = \text{Vi(t)} + \gamma_{1i}(\text{P}_i - \text{x}_i(t)) + \gamma_{2i}\,(\text{G}_i - \text{x}_i(t)) \quad (8)$$

Step 4 Update the Position, Xi (t + 1).

$$\text{Xij (t+1)} = \text{Xij (t)} + \text{Vij (t+1)} \quad (9)$$

where i is the particle index, j is the index of parameter of concern to be optimised, x is the position of the ith particle and jth parameter, k is the discrete time index, v is the velocity of the ith particle and jth parameter, P is the best position found by the ith particle and jth parameter (personal best), G is the best position found by swarm (global best), c is a random uniform number between [0,1] applied to the ith particle, u is the inertia function, a is the acceleration constants.

Step 5 Now; utilize the Fitness Function in order to evaluate the particle,

$$THD_V = \frac{\sqrt{\sum_{n=1}^{\infty} V_n^2}}{V_1} \quad (10)$$

For harmonic elimination. Here the switching angles $\alpha_1, \alpha_2, \alpha_3, \alpha_4, \alpha_5$, and α_6 are chosen in such a way that the selective harmonics 3th, 5th, 7th, 9th, and 11th is eliminated.

$$\text{F(1)}=(\cos(\alpha_1)+\cos(\alpha_2)+\cos(\alpha_4)+\cos(\alpha_4)+\cos(\alpha_5)+\cos(\alpha_6))\text{-ma};$$
$$\text{F(2)}=(\cos(3*\alpha_1)+\cos(3*\alpha_2)+\cos(3*\alpha_3)+\cos(3*\alpha_4)+\cos(3*\alpha_5)+\cos(3*\alpha_6));$$
$$\text{F(3)}=(\cos(5*\alpha_1)+\cos(5*\alpha_2)+\cos(5*\alpha_3)+\cos(5*\alpha_4)+\cos(5*\alpha_5)+\cos(5*\alpha_6));$$
$$\text{F(4)}=(\cos(7*\alpha_1)+\cos(7*\alpha_2)+\cos(7*\alpha_3)+\cos(7*\alpha_4)+\cos(7*\alpha_5)+\cos(7*\alpha_6));$$
$$\text{F(5)}=(\cos(9*\alpha_1)+\cos(9*\alpha_2)+\cos(9*\alpha_3)+\cos(9*\alpha_4)+\cos(9*\alpha_5)+\cos(9*\alpha_6));$$
$$\text{F(6)}=(\cos(11*\alpha_1)+\cos(11*\alpha_2)+\cos(11*\alpha_3)+\cos(11*\alpha_4)+\cos(11*\alpha_5)+\cos(11*\alpha_6)); \quad (11)$$

Step 6 Check the constraints $0 \le \alpha_1 \le \alpha_2 \le \alpha_3 \le \alpha_4 \le \alpha_5 \le \alpha_6 \le \pi/2$.

Step 7 Check for the case P(xi) < P(Pi), if i = i + 1 not satisfied then execute to Step 3.

Step 8 If the produced location of the particle is the best then update by change with the previous location as Pi =Xi.

Step 9 Update the global best location as Pg = min (P neighbour).

Step10 Switching angles are optimisedthe best. Accomplish the solution of the problem.

The general flow chart of PSO of a modified CHB-MLIs is shown in figure 8 and each step is explained below:

EXPERIMENTAL RESULTS OF CHB-MLIS (MI=0.81) USING NR AND PSO TECHNIQUES

The construction of the 13 levels of modified CHB-MLIs involves integrating the15 pieces of power switching semiconductor IGBTs- IHW30N90T with snubber circuits, respectively as shown in Figure-9. IGBT possessed the capability of operating up to 100 kHz switching frequency and in supplying electric current at 60 A at 25 ^{o}C, and in becoming 30 A when the temperature of the IGBTs reached 100 ^{o}C. Normally, it can operate at 600volt DC towards the break down voltage at 900volt DC. In this operation, the MI was set at 0.81 for both techniques with the calculation of switching angles of θ_1 =6.25^0, θ_2 =14.32^0,θ_3 =22.91^0, θ_4 =32.04^0, θ_5 =48.02^0, and θ_6 =62.64^{0}using NR and switching angles calculation of θ_1 =4.48^0, θ_2 =14.54^0,θ_3 =24.57^0, θ_4 =33.19^0, θ_5 =45.82^0, and θ_6 =62.67^0 using the PSO technique. By using the same method for the optimisation technique, the developed source codes using C language based on NR and PSO were stored in the DSP-TMS320F2812. In the thirteen-level model, there are three cells available in the configuration of a modified CHB-MLIs as shown in the methodology. The switches' timing diagrams at the duration of 0.02s with MI=0.81 using NR are illustrated in Figure-10 until Figure-12.

Figure-13 shows the output voltage waveform of a single-phase modified CHB-MLIs based on the NR technique. Figure-14 shows the optimisation harmonic spectrum of the output voltage waveform of a modified CHB-MLIs of thirteen levels with THD values equivalent to 6.3% using the NR technique.

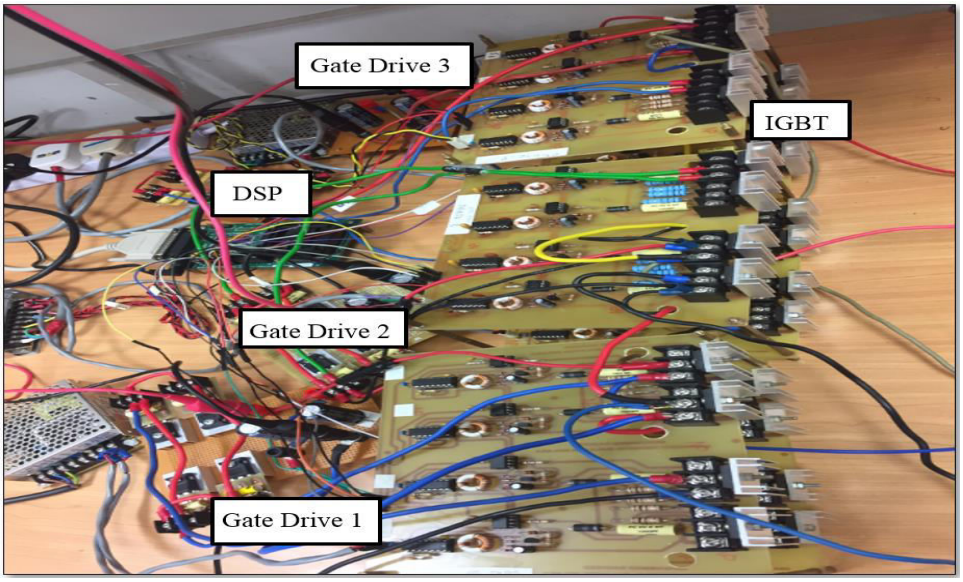

Figure-9. The development of a single-phase of modified CHB-MLIs for 13-levels.

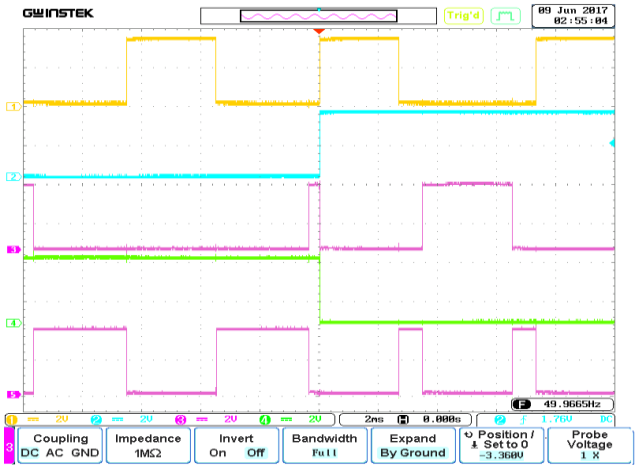

Figure-10. Switching pattern of a single-phase thirteen levels modified CHB-MLIs for cell one comprising S_1, S_2, S_3, S_4, and S_5 switches with MI=0.81 using NR technique.

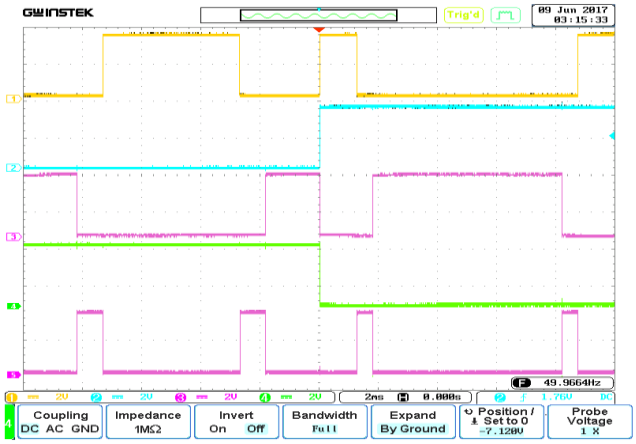

Figure-11. Switching pattern of a single-phase thirteen levels modified CHB-MLIs for cell two comprising S_6, S_7, S_8, S_9, and S_{10} switches with MI=0.81 using NR technique.

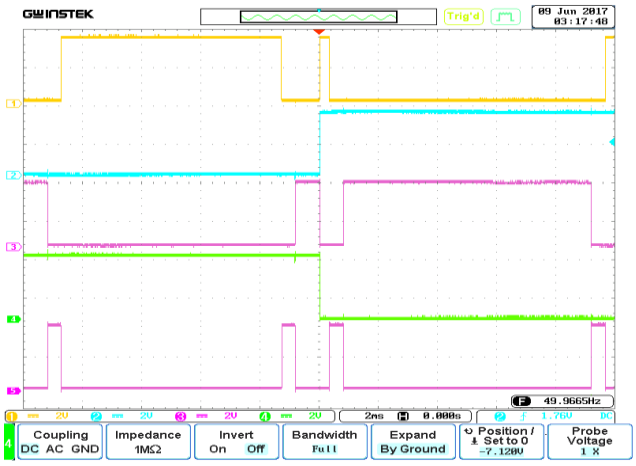

Figure-12. Switching pattern of a single-phase thirteen levels modified CHB-MLIs for cell three comprising S_{11}, S_{12}, S_{13}, S_{14}, and S_{15} switches with MI=0.81 using NR technique.

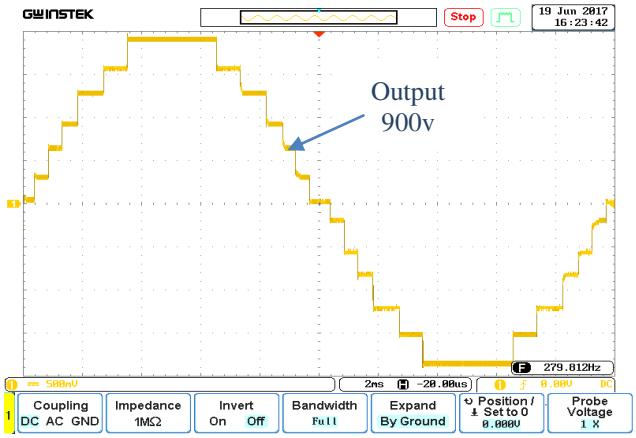

Figure-13. Output voltage waveform of a thirteen-level modified CHB-MLIs with MI=0.81 using NR technique.

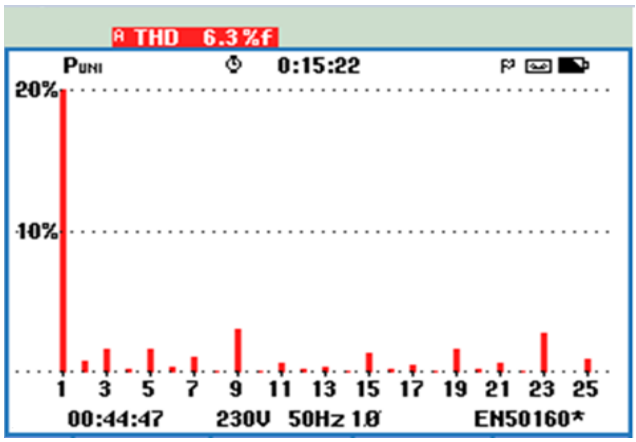

Figure-14. Harmonic spectrum of output voltage waveform of a modified CHB-MLIs with MI=0.81 using NR technique.

In the case of timing diagram using the PSO technique, the same MI value of 0.81 is used for a single-phase modified CHB-MLIs of thirteen levels, which can be observed in Figure-16 until Figure-18.

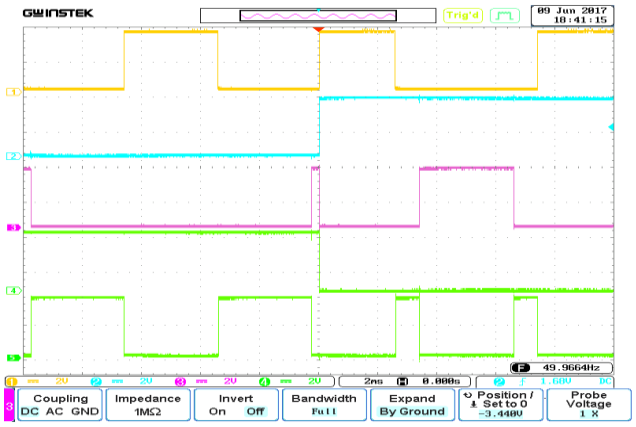

Figure-15. Switching pattern of a single-phase thirteen levels modified CHB-MLIs for cell one comprising S_1, S_2, S_3, S_4, and S_5 switches with MI=0.81 using PSO technique.

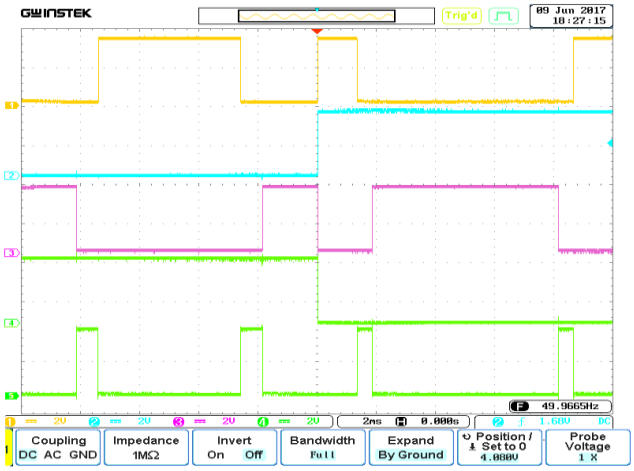

Figure-16. Switching pattern of a single-phase thirteen levels modified CHB-MLIs for cell two comprising S_6, S_7, S_8, S_9, and S_{10} switches with MI=0.81 using PSO technique.

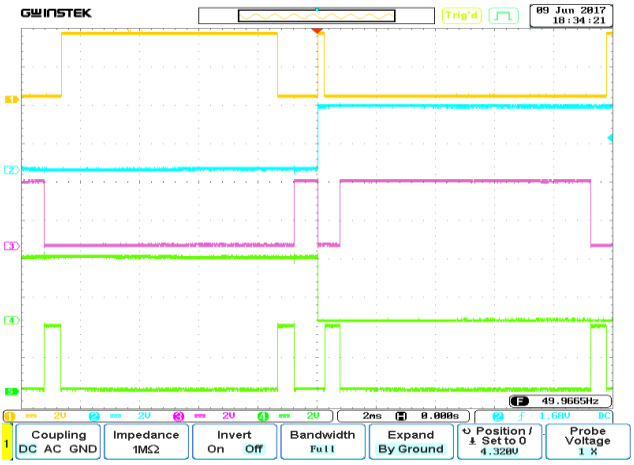

Figure-17. Switching pattern of a single-phase 13-levels modified CHB-MLIs for cell three comprising S_{11}, S_{12}, S_{13}, S_{14}, and S_{15} switches with MI=0.81 using PSO technique.

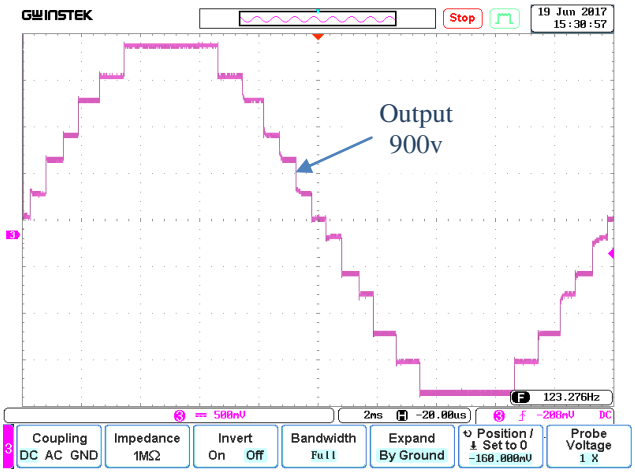

Figure-18. Output voltage waveform of a thirteen-level modified CHB-MLIs with MI=0.81 using PSO technique.

Figure-18 shows the optimisation of output voltage waveform of a modified CHB-MLIs based on the PSO technique. The optimisation of output voltage waveforms of a thirteen-level modified CHB-MLIs was smoother than nine and five levels. Figure-19 shows the optimisation harmonic spectrum of the output voltage waveform of a thirteen-level modified CHB-MLIs with THD values equivalent to 5.3% using the PSO technique. As shown in Figure-20, the values of THD for voltage is reduced using the PSO technique as compared to when using the NR technique.

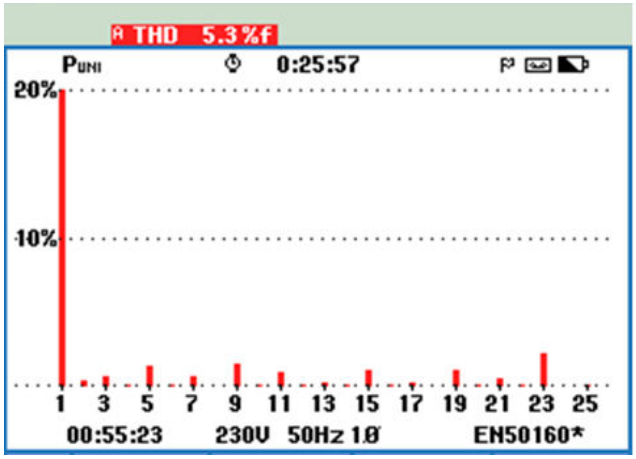

Figure-19. Harmonic spectrum of output voltage waveform of a modified CHB-MLIs with MI=0.81 using PSO technique.

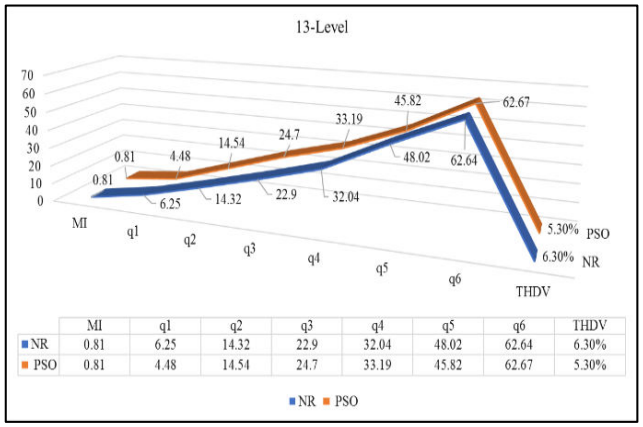

	MI	q1	q2	q3	q4	q5	q6	THDV
NR	0.81	6.25	14.32	22.9	32.04	48.02	62.64	6.30%
PSO	0.81	4.48	14.54	24.7	33.19	45.82	62.67	5.30%

Figure-20. Overall values of MI, versus the switching angles and the values of THD for voltage of modified CHB-MLI of 13-levelsbased on NR and PSO.

CONCLUSIONS

The experimental results showed that the higher level of inverter it will produce lower harmonics contents of the modified CHB-MLIs using the both techniques. However, PSO technique produce lower content of THD of the modified CHB-MLIs output voltage waveform compared to NR technique due to switching angles of the PSO technique is simple and efficient. The coding based on NR and PSO techniques were then stored into DSPTMS320F2812. The experimental results for the

optimization of single-phase modified CHB-MLIs of 13, levels are in good agreement with the experimental results, which further exhibit the effectiveness of the proposed developed prototype techniques in reducing harmonics.

ACKNOWLEDGEMENTS

This research is sponsored by the grant Penyelidikan Jangka Pendek (PJP) which the number is PJP/2019/FKE (2A)/S01668. The authors would also like to thank the Centre for Research and Innovation Management Universiti Teknikal Malaysia Melaka (CRIM-UTeM) for the funding to support this project to providing the facilities and research environment.

EFERENCES

[1] E. Babaei, M. F. Kangarlu, M. Sabahi and M. R. A. Pahlavani. 2013. Cascaded multilevel inverter using sub-multilevel cells. Electr. Power Syst. Res. 96: 101-110.

[2] H. Rashid. 2004. Power electronics: circuits, devices, and applications. Pearson/Prentice Hall.

[3] M. Jones and I. N. W. Satiawan. 2013. A simple multi-level space vector modulation algorithm for five-phase open-end winding drives. Math. Comput. Simul. 90: 74-85.

[4] S. K. Mondal, B. K. Bose, L. Fellow and V. Oleschuk. 2003. Space Vector Pulse Width Modulation of Three-Level Inverter Extending Operation into over modulation Region. IEEE Trans. POWER Electron. 18(2): 604-611.

[5] R. N. A. Krismadinata, H. W. Ping and J. Selvaraj. 2013. Elimination of Harmonics in Photovoltaic Seven-level Inverter with Newton-raphson Optimization. Procedia Environ. Sci. 17: 519-528.

[6] U. B. S. D. 2011. Harmonic Orientation of Pulse Width Modulation. Power Eng. Electr. Eng. 9(1): 29-34.

[7] A. Fri, R. El Bachtiri and A. El Ghzizal. 2013. A Comparative Study of Three Topologies of Three-phase (5L) Inverter for a PV System. Energy Procedia. 42: 436-445.

[8] O. Abdel-Rahim, H. Abu-Rub and A. Kouzou. 2013. Nine-to-Three Phase Direct Matrix Converter with Model Predictive Control for Wind Generation System. Energy Procedia. 42: 173-182.

[9] B. Boost, V. Current, S. Inverter, Q. Lei, S. Member and F. Z. Peng. 2014. Space Vector Pulse width Amplitude Modulation for a. 29(1): 266-274.

[10] E. Babaei, M. F. Kangarlu and F. N. Mazgar. 2012. Symmetric and asymmetric multilevel inverter topologies with reduced switching devices. Electr. Power Syst. Res. 86: 122-130.

[11] R.A Ahmed and S. Mekhilef. 2010. New multilevel inverter topology with minimum number of switches. TENCON 2010 - 2010 IEEE Reg. 10 Conf. pp. 1862-1867.

[12] S. H. H. Ebrahim Babaei. 2010. New multilevel inverter topology with minimum number of switches. IEEE Reg. 10 Annu. Int. Conf. Proceedings/TENCON. 50(11): 1862-1867.

[13] S. H. Hosseini, M. F. Kangarlu, and A. K. Sadigh. 2009. A New Topology for Multilevel Current Source Inverter with Reduced Number of Switches. Electr. Electron. Eng. 2009. ELECO 2009. Int. Conf. on. IEEE. pp. 273-277.

[14] W. A. Halim and N. A. Rahim. 2011. FPGA-based pulse-width modulation control for single-phase multilevel inverter. 2011 IEEE 1st Conf. Clean Energy Technol. CET 2011, pp. 57-62.

[15] J. J. Nedumgatt, D. V. Kumar, A. Kirubakaran and S. Umashankar. 2012. A multilevel inverter with reduced number of switches. 2012 IEEE Students' Conf. Electr. Electron. Comput. Sci. Innov. Humanit. SCEECS 2012. Vol. 1.

[16] 2011. Data sheet for super capacitor from EPCOS with Part No.: B48621-S0203-Q288.

[17] A. Al-janad, R. Omar, M. Rasheed, Z. Ibrahim and M. H. A. Mustapha. 2014. Analysing Performance of Super-Capacitor and Battery in Low Voltage Electrical. 61(1): 99-106.

[18] R. Vijayakumar. 2015. Selective Harmonic Elimination PWM Method using Seven Level Inverters by Genetic Algorithm Optimization Technique. Int. J. Eng. Res. Technol. 4(2): 812-818.

[19] A. K. Al-Othman and T. H. Abdelhamid. 2009. Elimination of harmonics in multilevel inverters with non-equal dc sources using PSO. Energy Convers. Manag. 50(3): 756-764.

[20] S. Sudha Letha, T. Thakur and J. Kumar. 2016. Harmonic elimination of a photo-voltaic based cascaded H-bridge multilevel inverter using PSO (particle swarm optimization) for induction motor drive. Energy. 107: 335-346.

[21] V. K. Gupta and R. Mahanty. 2015. Optimized switching scheme of cascaded H-bridge multilevel inverter using PSO. Int. J. Electr. Power Energy Syst. 64: 699-707.

[22] B. Alamri, A. Sallama and M. Darwish. 2015. Optimum SHE for Cascaded H-Bridge Multilevel Inverters Using : NR-GA-PSO, Comparative Study. pp. 1-10.